Propagation properties of fluxons in a well-damped Josephson transmission line

doi: 10.1063/1.333282

Propagation properties of fluxons in a well-damped Josephson transmission line

J. Nitta, A. Matsuda, and T. Kawakami
Musashino Electrical Communication Laboratory, Nippon Telegraph and Telephone Public Corporation, 3-9-11 Musashino-shi, Tokyo, 180 Japan

(Received 25 October 1983; accepted for publication 14 December 1983)

Fluxon threshold properties and propagation velocities have been studied with regard to Josephson transmission line (JTL) having an external shunt resistance parallel to the Nb/Nb-oxide/Pb junction. Stable and separated multifluxon waveforms have been observed in the well damped JTL. Experimentally obtained thresholds for the number of propagated fluxons and interval times between each respective fluxon agree with numerical simulations. The dependence of fluxon propagation velocities on the bias current level can be interpreted in terms of the McLaughlin–Scott theory.

PACS numbers: 74.50. + r, 74.60.Ge, 85.25. + k, 74.30.Gn

I. INTRODUCTION

Many applications[1–5] have been proposed of Josephson transmission lines (JTLs) to digital computer logic and memory functions. These have been based on the attractive feature that one quantized magnetic flux (fluxon) can be applied to one information bit. The fluxon propagates as a solitary wave (soliton) in the JTL, which can be described by the modified sine-Gordon equation,[6,7] including a damping term associated with quasiparticle tunneling loss and a distributed bias current term. The dependence of profiles for fluxon propagations on these additional terms has been investigated by means of numerical[4,8] and perturbation analyses.[9]

These analyses suggest that it is desirable to use well damped JTLs for digital applications, because of the following reasons.[4,8,9] In the case of a small damping parameter, the maximum bias parameter, above which separated fluxon formation does not occur, is limited. By increasing the damping effects, the fluxon rapidly reaches the final power-balance velocity, and stable fluxons are formed which include no vibration mode even if a step-like input is fed in. However, even with these promising features, a well damped JTL has not yet been realized, and, correspondingly, its fluxon propagation properties have not been observed. In the case of large damping and bias parameters where the perturbation approaches cannot be applied, it is thought to be instructive to investigate the fluxon propagation profiles experimentally.

This paper is an attempt to clarify the effect of damping and bias terms, as is the case of recent reports[10,11] by one of present authors, who described an observation of a single fluxon propagation by use of a minicomputer signal processing system, where the noise level reached and rise time are about 2 μV and 60 ps, respectively.

In Sec. II, JTL parameters and the well damped JTL structure are described. Section III describes the threshold properties and propagation velocities for fluxons investigated at various input voltage heights and bias current levels. The experimentally obtained properties are seen to agree with the theoretical results.

II. JTL PARAMETERS AND STRUCTURE

The JTL, including the quasiparticle tunneling loss and distributed bias current, can be described by the following normalized nonlinear differential equation:

$$\frac{\partial^2\varphi}{\partial x^2} - \frac{\partial^2\varphi}{\partial t^2} = \sin\varphi + \alpha\frac{\partial\varphi}{\partial t} - \gamma, \tag{1}$$

where length and time are normalized by Josephson penetration depth $\lambda_j = (\Phi_0/2\pi\mu_0 d j_c)^{1/2}$ and Josephson plasma period $\tau_j = (\Phi_0\epsilon/2\pi j_c t_{0x})^{1/2}$ (Φ_0 is flux quantum, t_{0x} tunnel barrier thickness, J_C maximum Josephson current density, ϵ the tunnel barrier dielectric constant and $d = 2\lambda_L + t_{0x}$; λ_L is the London penetration depth for both electrodes), respectively. Damping and normalized bias parameters are, respectively, determined by the relations $\alpha = (\Phi_0 t_{0x}/2\pi j_c\epsilon)^{1/2}/r$ and $\gamma = j_B/j_C$, where r is the quasiparticle tunneling resistance per unit length, and j_B the distributed bias current per unit length.

The damping parameter α suggests that a well damped JTL can be realized either by the addition of external shunt resistance $R_D \ll r$ or by a reduction in maximum Josephson current density (with a conventional JTL, $\alpha = 0.004$ is obtained as a damping parameter value for $j_C = 3.6$ A/cm^2, because of the large r tunneling resistance value[11]). The latter method, however, causes the effective JTL length to become shorter. Accordingly, a JTL with a Cr external shunt resistance parallel to the junction and Au input termination resistance, was fabricated by the conventional fabrication technique.[10] The JTL (50-μm width and 1-cm length) was an Nb/Nb-oxide/Pb tunnel junction in an overlapping geometry, as shown in Fig. 1(a). Note that, in Fig. 1(a), an Au layer is used as contact layer between the Pb upper electrode and Cr damping resistance.

Figure 1(b) shows an equivalent circuit. Termination resistance R_T at the input end acts to supply effective input voltage to the JTL. It is approximately set at $R_T = Z_0$ ($= 0.028\ \Omega$), where Z_0 is characteristic impedance for the JTL. External shunt resistance R_D per unit length was attached to the vicinity of the tunnel junction, so as to eliminate any inductance component. Comb-like electrodes were used to maintain homogeneous bias feeding.

 0021-8979/84/072758-05$02.40

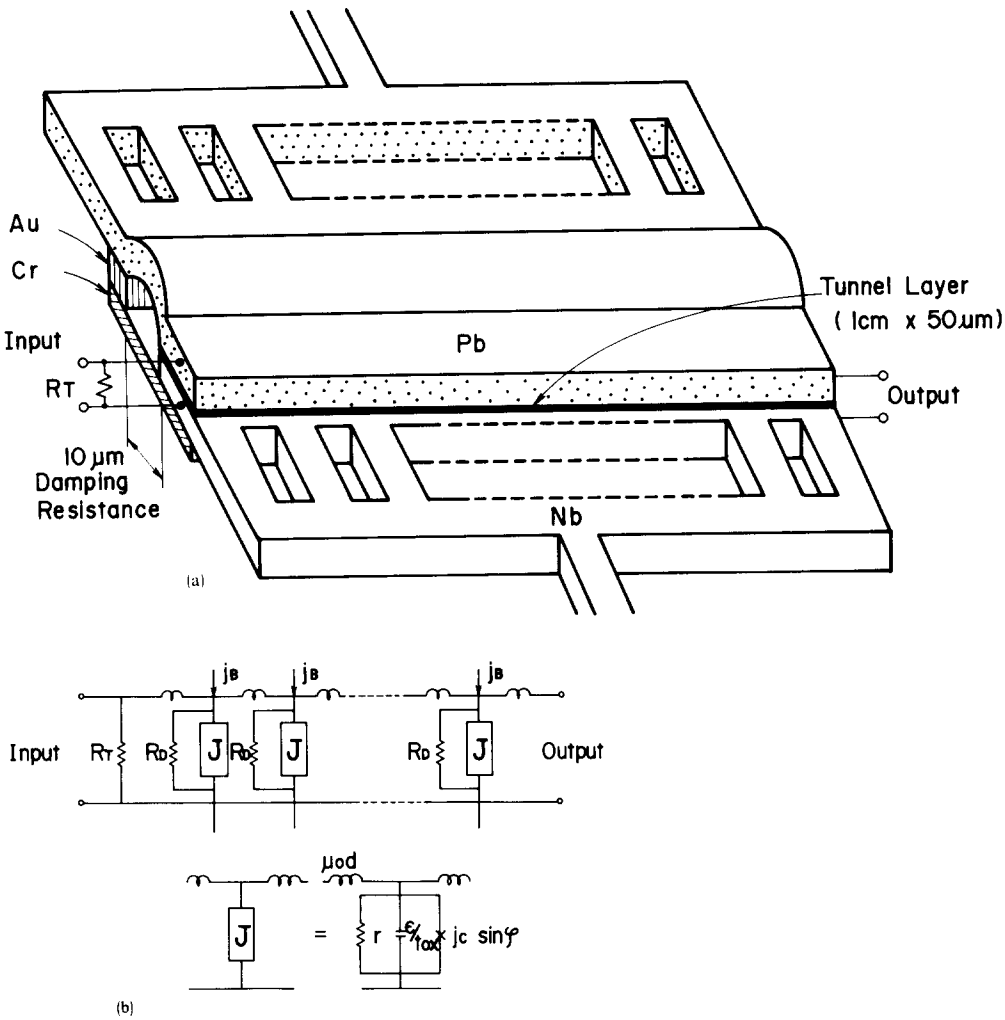

FIG. 1. Fabricated JTL structure: (a) block diagram representing Nb/Nb-oxide/Pb junction and Cr damping resistance. Au layer is used as contact layer between Pb upper electrode and Cr damping resistance; (b) equivalent circuit.

The maximum Josephson current density was determined to be $J_C = 0.67$ A/cm^2 using the I-V characteristics for the JTL as gleaned from the bias electrodes shown in Fig. 2. Josephson penetration depth and plasma period were estimated at $\lambda_j = 552\,\mu$m and $\tau_j = 64$ ps, respectively. The fabricated JTL length corresponds to 18 λ_j. The damping parameter was determined to be $\alpha = 0.66$ using the normal resistance component of the JTL's I-V characteristics. This method is rather exact, because the external shunt resistance was much smaller than the termination resistance. The termination resistance was indirectly determined to be $R_T = 0.8\,Z_0$ through the use of Au monitor resistance in the JTL vicintiy.

III. FLUXON PROPAGATIONS PROPERTIES

A. Input pulse height threshold for propagated fluxon number

Output voltage responses were measured at another open end of the JTL at the moment when input voltage pulses were fed to the termination resistance. The measurement system used for observation of single fluxon propagation has previously been described in Ref. 10. The input voltage waveform at an attenuation of 0 dB is shown in Fig. 3(a). Examples of observed output pulse waveforms with a fixed bias current of 1.8 mA ($\gamma = 0.545$) are shown in Fig. 3(b), as a

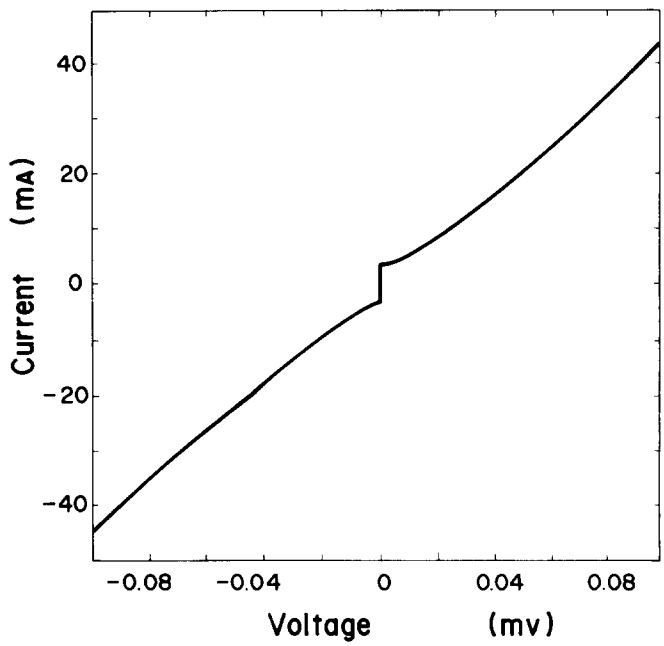

FIG. 2. JTL I-V characteristics. Normal resistance corresponds to external shunt resistance.

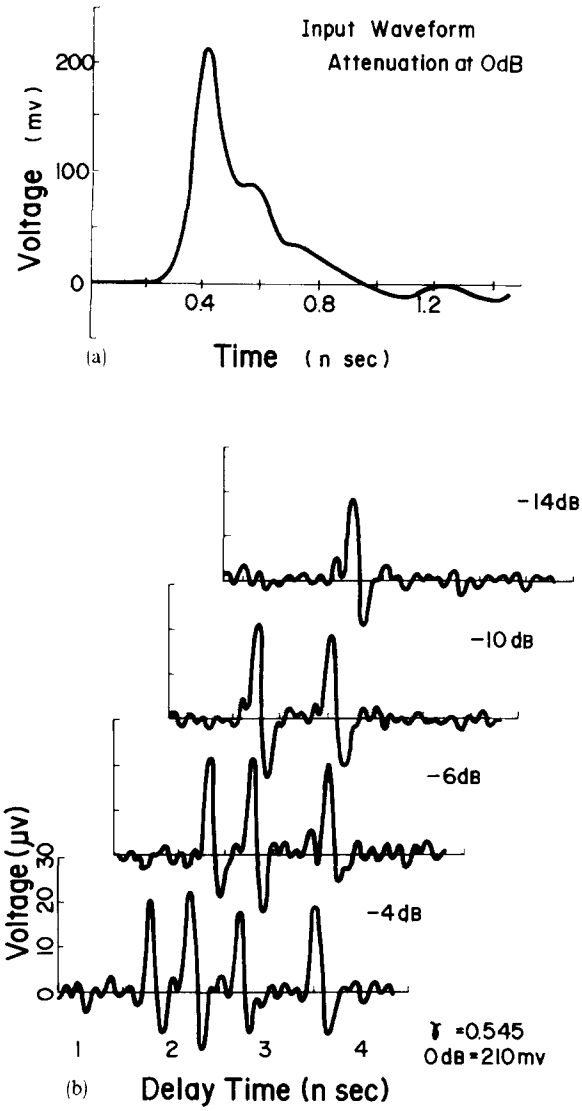

FIG. 3. Pulse waveform: (a) input at 0 dB; (b) output profiles as function of input pulse height with fixed bias of $\gamma = 0.545$.

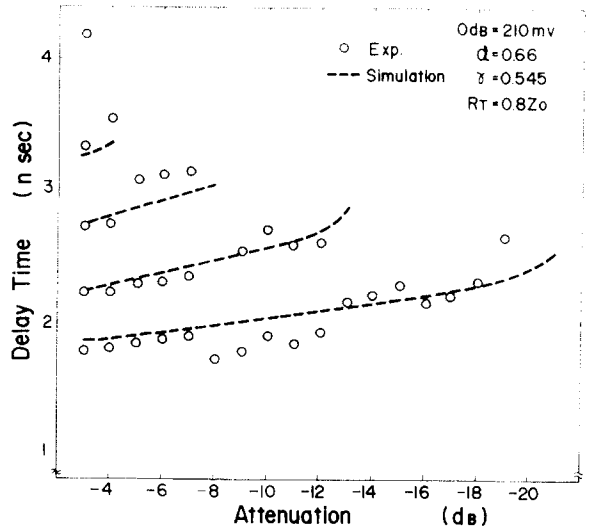

FIG. 4. Propagation delay times for respective fluxon peak positions as function of input pulse height with fixed bias of $\gamma = 0.545$. Open circles and broken lines indicate experimental results and numerical simulation, respectively.

parameter of the attenuation value of input voltage. Although a single input pulse was fed in, a group including well separated pulses which had approximately the same 20-μV height and 100-ps width was observed at the output end. These observed features ensure that each output voltage pulse corresponds to a single fluxon ($\Phi_0 = 2.07 \times 10^{-15}$ Vs). Results also indicate that the propagated fluxons were not reflected as antifluxons at the open end. Whether the reflection occurs or not will be referred to again in the discussions below. With a decrease in input pulse height, the output fluxon number also decreased. Any propagated fluxons could not be observed below $-$ 20 dB.

Figure 4 shows that transmission delay times of the separated fluxons from the input pulse peak are plotted as a function of input pulse height with a normalized bias of $\gamma = 0.545$. To compare experimentally obtained results with simulated results, Eq. (1) was numerically integrated by using a real input waveform, an appropriate boundary condition, and the JTL parameters obtained in Sec. II. According to the results of simulation using $\alpha = 0.66$ and $\gamma = 0.545$, it does not occur throughout the input pulse level that propagated fluxons were reflected as antifluxons at the open end. It should be noted that in Fig. 4 open circles and broken lines indicate experimental and simulated results, respectively. The experimentally obtained threshold values for the propagated fluxon number and interval times between the respective fluxons agree with the simulation results.

In the present numerical simulations, an output pulse with 2 Φ_0 ($= \int V \cdot ds$), which corresponds to two fluxons, could be observed if the reflection might occur as an antifluxon at the open end. By increasing the bias level for an input pulse of $-$ 15 dB, and $\alpha = 0.66$, propagated fluxons were reflected as antifluxons above $\gamma = 0.788$. These numerical results do not agree with the results of perturbation theory[9] because of the large α and γ values beyond the perturbation approaches. In the present experiments, on the other hand, antifluxon reflections could not be observed under high bias conditions ($\gamma > 0.8$). This discrepancy is not yet understood and will be subjects for future study.

B. Propagation velocity dependence on bias current

Fluxon propagation delay times for various fixed input pulse heights were measured as a function of normalized bias current. Figure 5 shows a comparison of propagation delay times between the nondamped JTL[11] and the well damped JTL. Open circles and triangles indicate the experimental first fluxon delay times for the well damped JTL at $-$ 10 and $-$ 15 dB attenuations, respectively. Dots indicate the delay times of the nondamped JTL ($\alpha = 0.0041$) at $-$ 13 dB.[11]

With an increase of the bias current, the delay time of the well damped JTL decreased. However, in the nondamped JTL, stable and separated fluxon propagations could not be held for $\gamma > 0.5$, and voltage transitions occurred for $\gamma > 0.7$.[11] On the other hand, stable fluxon propa-

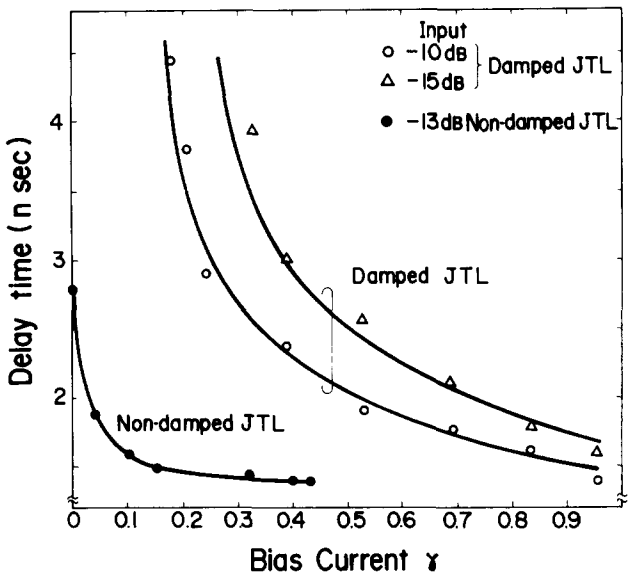

FIG. 5. Comparison of propagation delay times between well damped JTL and nondamped JTL. Open circles and triangles indicate experimental delay times for well damped JTL with − 10- and − 15-dB attenuations, respectively. Dots indicate experimental delay times for nondamped JTL at − 13 dB.[11]

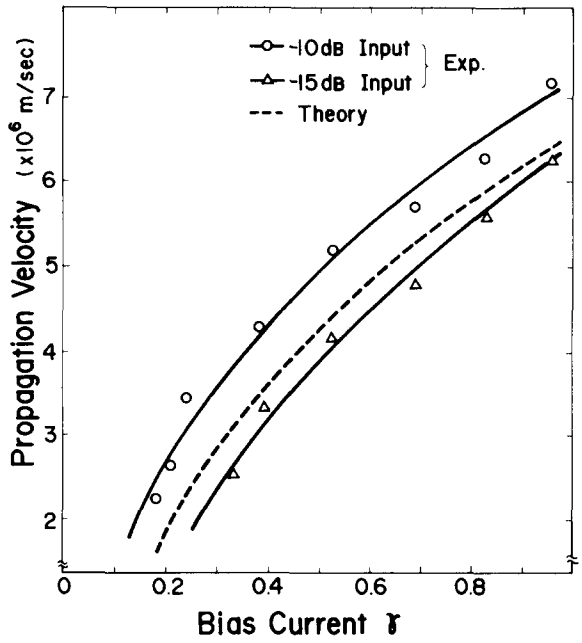

FIG. 6. Comparison of fluxon propagation velocities between experimentally obtained results and the McLaughlin–Scott theory. Open circles and triangles indicate experimental results for − 10- and − 15-dB attenuations, respectively. Broken line indicates theoretical final velocities.

gations were observed under the high bias condition in the present well damped JTL. The delay times also varied throughout almost all bias current levels.

It has been reported that, with a small damping parameter, propagated fluxons bunch together and many fluxons are created by an increase in the bias level.[8] For a large damping parameter, on the other hand, stable and separated fluxon propagations occur under high bias condition.[4,8] These experimentally obtained results verify the numerical simulations,[4,8] and indicate that the delay time can be easily controlled by manipulation of the bias current level in a well damped JTL.

The dependence of fluxon propagation velocity on the bias and damping parameters was investigated. According to numerical[4,8] and theoretical analyses,[9] the bias current and damping terms cause fluxons to accelerate and to slow down, respectively. McLaughlin–Scott were able to obtain the final power-balance velocity, where the fluxon energy injected by the bias current was balanced by the quasiparticle tunneling loss.[9]

Figure 6 shows a comparison of velocities between experimentally obtained results and theoretical velocities. The experimental average velocities could be directly calculated from the fluxon propagation delay times and fabricated JTL length. Theoretical final velocities were estimated with the use of the McLaughlin–Scott equation[9]

$$u = u_0\left[1+\left(\frac{4\alpha}{\pi\gamma}\right)^2\right]^{-1/2}. \tag{2}$$

Here, the maximum propagation velocity was $u_0 = 8.3\times 10^6$ m/s for the present JTL. In Fig. 6, open circles and triangles indicate the experimentally obtained velocities for − 10 and − 15 dB, respectively. A broken line indicates the theoretical final velocities. The experimental average velocities, including initial velocities after fluxon formation, seems to agree with the final velocities approximately. This agreement can be regarded as a feature of a well damped JTL, where the fluxon rapidly reaches the final power-balance velocity. The difference in velocities between the − 10- and − 15-dB input cases indicates that the higher input pulse heights provide fluxons with faster initial velocities.

C. Fluxon formation process

The fluxon formation process was also simulated, in order to investigate the features of a well damped JTL under various damping and bias parameters. Figure 7 shows a current distribution curve ($-\partial\varphi/\partial x$) on a space-time ($x$-$t$) plane for a damping parameter of $\alpha = 0.66$, a normalized bias of

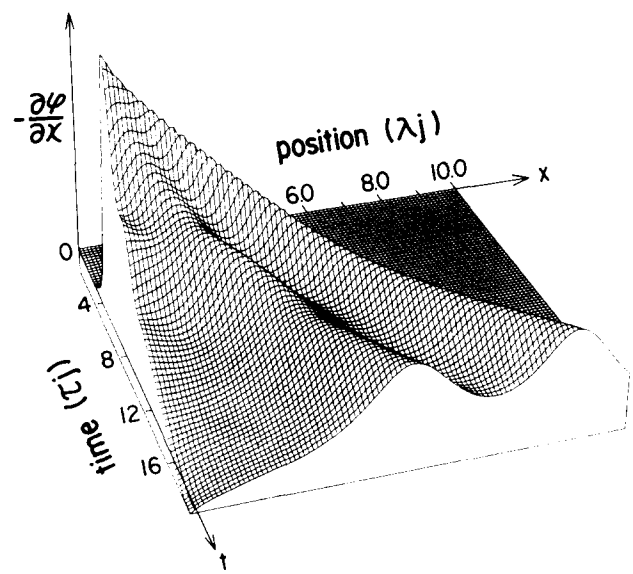

FIG. 7. Current distribution curve ($-\partial\varphi/\partial x$) on space-time ($x$-$t$) plane for $\alpha = 0.66$, $\gamma = 0.545$ and input pulse of − 10 dB. Space and time coordinates are normalized by Josephson penetration depth (552 μm) and Josephson plasma period (64 ps), respectively. Position $x = 0$ corresponds to input termination.

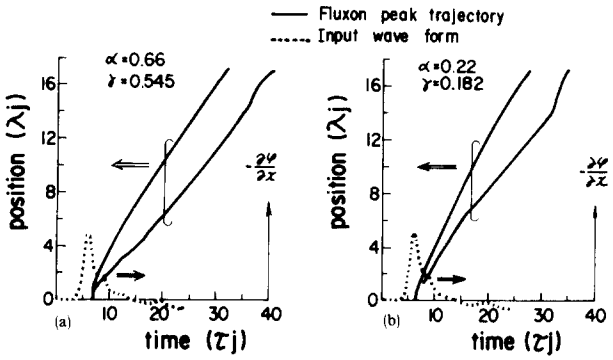

FIG. 8. Fluxon peak trajectories on space-time (x-t) plane. Broken line indicates input wave. Positions $x = 0$ and $x = 18\ \lambda_j$ correspond to input and output terminations, respectively. (a) $\alpha = 0.66$, $\gamma = 0.545$ and input of -10 dB; (b) $\alpha = 0.22$, $\gamma = 0.182$ and input of -10 dB.

$\gamma = 0.545$, and an input pulse of -10 dB. The current distribution at the JTL input end ($x = 0$) indicates the effective applied input current. As time passes, the current distribution peak at the input end splits up into two peaks having different initial velocities. The respective peaks, which correspond to two fluxons, gradually broaden and approach the final power-balance velocities.[9] Finally, the sufficiently split and stable fluxons propagate in the well damped JTL.

The trajectories for each respective fluxon peak are plotted on an x-t plane for $\alpha = 0.66$, $\gamma = 0.545$ and an input pulse of -10 dB in Fig. 8(a). In Fig. 8(b), a reduced damping case for $\alpha = 0.22$, $\gamma = 0.182$ and an input of -10 dB is shown. Here, damping and bias parameters were chosen to keep the final power-balance velocity constant (the ratio α/γ is constant). The input pulse peak splits up into first and second fluxons having different velocities.

Simulation results indicate that, for $\alpha = 0.66$, the first fluxon approximately reaches the final velocity after $10\ \tau_j$. However, for $\alpha = 0.22$, the propagation velocity is still faster than the final velocity even after $20\ \tau_j$. It is interesting to note that, with a decrease in the damping effects, the initial velocities for the respective fluxons increase, and, on the contrary, the difference between the initial velocities decreases. Short-range interactions during the splitting process may be thought of as more prominent for large damping cases than for small cases.

Near the open output end, abnormal behavior is observed for the secondary fluxons. Their velocities abruptly increase for both cases ($\alpha = 0.22$ and $\alpha = 0.66$). This can be explained in terms of an attractive force between the secondary fluxon and an antifluxon-like wave, which originates from the incomplete reflection of the first fluxon at the open output end. The antifluxon-like wave, which is small and not quantized, soon decays during its propagation.

IV. CONCLUSION

Threshold properties and propagation velocities for fluxons were investigated both experimentally and theoretically for a well damped JTL. The JTL was fabricated together with an external shunt resistance parallel to the Nb/Nb-oxide/Pb junction. Stable and well separated fluxon propagations were observed, even if a high bias current was fed in. The experimentally obtained threshold for the number of propagated fluxons and interval times between each respective fluxon agree with the computer simulations. The dependence of fluxon propagation velocity on bias current level could be interpreted in terms of the McLaughlin–Scott theory. The advantages of a well damped JTL in regard to the digital applications exist in the fact that completely separated fluxon formation occurs and that the delay times can be easily controlled by the bias current level.

ACKNOWLEDGMENTS

The authors would like to express their thanks to N. Kuroyanagi and H. Okamoto for their continuous support, and to H. Takayanagi, K. Kuroda, and K. Hohkawa for their kind advice.

[1] T. A. Fulton, R. C. Dynes, and P. W. Anderson, Proc. IEEE **61**, 28 (1973).
[2] P. Gueret, Trans. IEEE Magn. **MAG-11**, 751 (1975).
[3] K. Nakajima, Y. Onodera, and Y. Ogawa, J. Appl. Phys. **47**, 1620 (1976).
[4] A. Matsuda and H. Yoshikiyo, J. Appl. Phys. **52**, 5727 (1981).
[5] V. Rajeevakumar, Trans. IEEE Magn. **MAG-17**, 591 (1981).
[6] A. C. Scott, Nuovo Cimento B **69**, 241 (1970).
[7] A. C. Scott, F. Y. F. Chu, and S. A. Reible, J. Appl. Phys. **47**, 3272 (1976).
[8] K. Nakajima, Y. Onodera, T. Nakamura, and R. Sato, J. Appl. Phys. **45**, 4095 (1974).
[9] D. W. McLaughlin and A. C. Scott, Appl. Phys. Lett. **30**, 545 (1977); Phys. Rev. A **18**, 1652 (1978).
[10] A. Matsuda and S. Uehara, Appl. Phys. Lett. **41**, 770 (1982).
[11] A. Matsuda and T. Kawakami, Phys. Rev. Lett. **51**, 694 (1983).